Science of the Total Environment 870 (2023) 161925

Contents lists available at ScienceDirect

Science of the Total Environment

journal homepage: www.elsevier.com/locate/scitotenv

Agricultural practices drive elevated rates of topsoil decline across Kenya, but terracing and reduced tillage can reverse this

Christopher J. Feeney [a,*], David A. Robinson [a], Amy R.C. Thomas [a], Pasquale Borrelli [b], David M. Cooper [a], Linda May [c]

[a] UK Centre for Ecology & Hydrology, Environment Centre Wales, Deiniol Road, Bangor, Gwynedd LL57 2UW, UK
[b] Department of Science, Roma Tre University, Viale Guglielmo Marconi, 446, 00146 Rome, Italy
[c] UK Centre for Ecology & Hydrology, Bush Estate, Penicuik, Midlothian EH26 OQB, UK

HIGHLIGHTS

- Modern land cover patterns drive elevated soil & nutrient loss rates across Kenya.
- Model & compare erosion rates for present with potential natural vegetation cover
- >300 Mt yr^{-1} of soil to be lost nationally; 5 % of topsoil to be lost in <100 years.
- Highest erosion rates in croplands; >25 % will lose top 20 cm of soil in <100 years.
- Reduced tillage and building terraces eliminate elevated cropland soil loss rates.

GRAPHICAL ABSTRACT

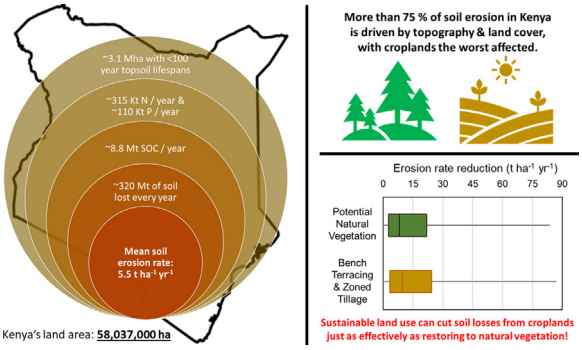

ARTICLE INFO

Editor: Manuel Esteban Lucas-Borja

Keywords:
Soil erosion
Topsoil lifespan
Lateral nutrient flux
Potential natural vegetation
Agricultural support practices
Modelling

ABSTRACT

As agricultural land area increases to feed an expanding global population, soil erosion will likely accelerate, generating unsustainable losses of soil and nutrients. This is critical for Kenya where cropland expansion and nutrient loading from runoff and erosion is contributing to eutrophication of freshwater ecosystems and desertification. We used the Revised Universal Soil Loss Equation (RUSLE) to predict soil erosion rates under present land cover and potential natural vegetation nationally across Kenya. Simulating natural vegetation conditions allows the degree to which erosion rates are elevated under current land use practices to be determined. This methodology exploits new digital soil maps and two vegetation cover maps to model topsoil (top 20 cm) erosion rates, lifespans (the mass of topsoil divided by erosion rate), and lateral nutrient fluxes (nutrient concentration times erosion rate) under both scenarios. We estimated the mean soil erosion rate under current land cover at ~5.5 t ha^{-1} yr^{-1}, ~3 times the rate estimated for natural vegetation cover (~1.8 t ha^{-1} yr^{-1}), and equivalent to ~320 Mt yr^{-1} of topsoil lost nationwide. Under present erosion rates, ~8.8 Mt, ~315 Kt, and ~ 110 Kt of soil organic carbon, nitrogen and phosphorous are lost from soil every year, respectively. Further, 5.3 % of topsoils (~3.1 Mha), including at >25 % of croplands, have short lifespans (<100 years). Additional scenarios were tested that assume combinations of terracing and reduced tillage practices were adopted on croplands to mitigate erosion. Establishing bench terraces with zoned tillage could reduce soil losses by ≥75 %; up to 87.1 t ha^{-1} yr^{-1}. These reductions are comparable to converting croplands to natural vegetation, demonstrating most agricultural soils can be conserved successfully. Extensive long-term monitoring of croplands with terraces and reduced tillage established is required to verify the efficacy of these agricultural support practices as indicated by our modelling.

* Corresponding author.
E-mail address: chrfee@ceh.ac.uk (C.J. Feeney).

http://dx.doi.org/10.1016/j.scitotenv.2023.161925
Received 14 October 2022; Received in revised form 26 January 2023; Accepted 27 January 2023
Available online 31 January 2023

1. Introduction

Soil has been described as the most essential natural resource for human security in the 21st century (Amundson et al., 2015) owing to the multitude of ecosystem services and goods it provides, including air and water purification, a major habitat for terrestrial biodiversity, and a fertile medium for food production (MEA, 2005). Soil erosion by water is one of the major pathways causing degradation of this essential resource, along with soil organic carbon (SOC) loss, vegetation degradation, aridity and salinization (Prăvălie, 2021). The erosion of fertile topsoil will have deleterious consequences for land productivity and the total environment through degradation of soil and vegetation structure and loss of key nutrients such as carbon (C), nitrogen (N) and phosphorous (P) (e.g. Alewell et al., 2020; Bakker et al., 2005), with knock-on effects on food security as crop yields decline (e.g. Pimentel and Burgess, 2013; Smaling et al., 2015). Moreover, the erosion of soil has implications for global carbon cycling and climate change as soils lose organic carbon more rapidly as carbon dioxide to the atmosphere and become less able to store carbon in future (Lugato et al., 2018; Van Oost et al., 2007). There will be implications for water quality also as more topsoil nutrients and sediment are washed into freshwaters, making these environments increasingly deprived of oxygen and toxic to fish (e.g. McCool and Renard, 1990; Rickson, 2014).

Current rates of annual soil loss by water are estimated at 28–36 Pg yr^{-1} worldwide (Borrelli et al., 2017; Quinton et al., 2010) and, in croplands, erosion rates exceed soil formation rates by factors of 10 to 40 (Pimentel and Burgess, 2013). A global synthesis of measured erosion and formation rates revealed that one third of topsoils have lifespans (defined as the time for a soil profile to erode away) of <200 years (Evans et al., 2020). These figures, together with the finding that one third of soils globally are degraded from erosion, aridity, pollution, organic carbon depletion and salinization (FAO and ITPS, 2015), highlight the immediate threat that erosion poses to soil sustainability worldwide.

Soil erosion perturbs biogeochemical cycles, namely of SOC N and P. This is particularly important as SOC, N and P are key indicators of soil health owing to their close associations with several physical, chemical and biological aspects of soil structure such as plant nutrient availability and organic matter content (Mosier et al., 2021). Quinton et al. (2010) estimated the magnitudes of N and P losses by soil erosion (referred to herein as "lateral nutrient fluxes") to be comparable to fluxes associated with crop uptake and fertiliser application. More recent analysis suggests that soil erosion is responsible for half of all P losses from the top 30 cm of soil globally (Alewell et al., 2020). The effects of soil erosion on SOC cycling are highly complex; for example, the mobilisation of soil could increase mineralisation rates of SOC, leading to losses of >20 % of total SOC as carbon dioxide (Lal, 2003). It has however, also been claimed soil erosion may induce a net carbon sink (Sanderman and Berhe, 2017; Van Oost et al., 2007), though this is disputed (Lugato et al., 2018).

Mitigating soil erosion requires an understanding of how much of it is driven by current land use practices. One method is to calculate differences in process rates between present-day conditions and under historical or "potential natural vegetation" (PNV) conditions where human activity is absent (as suggested by Wuepper et al., 2021). In so doing, the scale of the change necessary to reduce soil erosion and its associated effects can be identified to better target interventions (Zhao et al., 2021). Importantly, by comparing estimated contemporary process rates with estimated rates under PNV, one obtains a benchmark with which to contextualise the effectiveness of interventions to mitigate soil erosion. Such an assessment could integrate topsoil properties that are affected directly by erosion: topsoil lifespans and lateral fluxes of SOC, N and P (Wuepper et al., 2021). This approach is arguably appropriate, as the top three threats to soil functions globally include soil erosion, SOC loss and nutrient imbalance (Montanarella et al., 2016).

Previous assessments have revealed that Africa is the continent most impacted by soil erosion (Batjes, 1996; Borrelli et al., 2017; García-Ruiz et al., 2015) including some of the highest losses of C, N and P driven by this process (Alewell et al., 2020; Lal, 2003; Quinton et al., 2010). Further, sub-Saharan Africa has the second shortest median recorded topsoil lifespan (671 years), behind North America at 583 years (Evans et al., 2020). The high soil erosion potential of the humid tropics portion of sub-Saharan Africa is driven by heavy rainfall that is concentrated typically during two rainfall seasons in the Spring and Autumn months of each year (Labrière et al., 2015). Fenta et al. (2020) meanwhile, have highlighted that even in arid areas, water erosion risk can still be significant. Compounding climate drivers are rapid land cover changes (deforestation, cropland expansion, urbanisation and agricultural intensification), as most human population growth currently occurs in the tropics (Hartemink et al., 2008). This high susceptibility to soil erosion is expected to continue to be reflected in future, with up to 66 % higher soil erosion rates by 2070 according to recent simulations of 21st Century land use and climate change projections (Borrelli et al., 2020).

For this study, we sought to test the following hypotheses: (i) Present-day soil erosion rates are elevated because of modern land cover patterns, with erosion being the most severe on croplands; (ii) land management interventions on croplands, referred to herein as "agricultural support practices", can reduce elevated soil erosion rates on croplands back to natural baseline levels. Here, we provide quantitative estimates of gross soil erosion rates across Kenya, through the application of a high-resolution, spatially distributed modelling approach. We exploit several spatial datasets published in recent years to predict the lifespans of topsoil and lateral fluxes of SOC, N and P resulting from erosion, thereby providing an integrated analysis of both soil erosion risk and its consequences for topsoil health. Maps of present-day land cover and PNV are used to drive modelling of erosion rates under these two scenarios. Subtracting predicted conditions under natural vegetation from present-day land cover establishes how elevated current soil erosion rates are compared to a set of natural baseline conditions. Through statistical modelling, we map out smaller regions of Kenya, representing unique zones of interactions among the controls on lateral nutrient fluxes associated with soil erosion. In doing so, we not only develop our understanding of local controls on nutrient losses, but also produce a framework, whereby interventions to alleviate land degradation from soil erosion can be better targeted. Demonstrating this, we then model scenarios of agricultural support practices, to quantify how much of the elevated soil erosion rates could be reversed on croplands.

2. Materials and methods

2.1. Overview and data sources

We used the Revised Universal Soil Loss Equation (RUSLE) (Renard et al., 1997; Wischmeier and Smith, 1978) to predict gross soil erosion rates caused by water across Kenya (see Text S1; Supplementary Materials for a detailed summary). RUSLE computes soil losses through sheet-wash, rill and inter-rill processes within a defined area. The model is empirical and incorporates five risk factors: Rainfall-Runoff Erosivity (R; MJ mm ha^{-1} h^{-1} yr^{-1}), Soil Erodibility (K; t ha h ha^{-1} MJ^{-1} mm^{-1}), Slope Length and Steepness (LS; unitless), Cover-Management (C; unitless), and Support Practices (P; unitless). It estimates gross soil erosion rate (A; t ha^{-1} yr^{-1}) as follows:

$$A = R \times K \times LS \times C \times P \quad (1)$$

RUSLE was chosen for several important advantages: (1) it is a simple, physically plausible empirical model that provides reasonably accurate estimates for large-scale studies and most practical purposes; (2) previous application of RUSLE at national, continental and global scales has already been demonstrated (e.g. Borrelli et al., 2017; Panagos et al., 2015) including in Kenya (e.g. Watene et al., 2021); (3) newly available large scale and fine spatial resolution datasets covering Africa can be used to calculate RUSLE's component factors; (4) its empirical nature means that the RUSLE model does not require calibration, allowing rapid calculation of soil loss rates under multiple scenarios; and

(5) additional outputs can be derived from RUSLE modelling, including estimated topsoil lifespans and lateral fluxes of soil-associated nutrients.

A core objective of our study was to estimate the extent to which soil erosion rates under current land use are elevated compared to natural vegetation conditions. Therefore, we needed to create two soil erosion maps of Kenya: one based on current land cover; another based on the spatial distribution of natural vegetation cover that could occur given present-day climatic and edaphic conditions (Fig. 1).

Spatial datasets, including digital soil maps (DSMs) of topsoil properties (SOC, total N, extractable P, clay, silt, sand, USDA texture class, bulk density and stone content), soil profile data, land cover maps, a digital elevation model (DEM), and raster layers representing rainfall volumes, were compiled from the ISDA soil database (iSDA, 2022) and links listed in the paper that describe the production of the DSMs (Hengl et al., 2021). These datasets were chosen because (except for the 1 km SM2RAIN rainfall data) they are all 30 m spatial resolution and would allow us to produce the finest resolution predictions of soil erosion for Kenya. All raster layers were clipped to the Kenya shapefile taken from the "1:10m Cultural Vectors" published by Natural Earth (Natural Earth, 2022). The ISDA soil website hosts predicted soil properties at two depth intervals: 0–20 cm and 20–50 cm (iSDA, 2022). We modelled losses from the topsoil only and so the term "topsoil" herein refers to the top 20 cm of soil unless stated otherwise. Two land cover maps were used for the soil erosion modelling: The Copernicus Africa Land Cover 2016 map to represent present-day land cover; and the Kenyan portion of the Potential Natural Vegetation (PNV) Map of East Africa (van Breugel et al., 2015) to represent natural vegetation conditions. The two land cover maps were harmonised by reclassifying their vegetation/land cover to aggregated categories of the International Geosphere-Biosphere Programme (IGBP) classes (Fig. 1) prior to computation of C-factor and soil erosion rates (see Text S1; Supplementary Materials). All layers were re-projected to the WGS 1984 Lambert Azimuthal Equal Area coordinate reference system, commonly used for East Africa. The 1 km rainfall raster layers were exported from ArcMap 10.6.1 to new GeoTiff files with a 30 m resolution without statistical downscaling. Vector datasets such as the Food and Agriculture Organisation Digital Soil Map of the World (FAO DSMW) (FAO, 1977) and the PNV map were rasterised to 30 m grids and exported as new GeoTiffs. Additionally, monitored soil erosion rates and topsoil lifespans estimated from these were amassed from existing literature to evaluate model performance. Details on the soil erosion model evaluation, uncertainty analysis and sensitivity to component variables are provided in Text S2 (Supplementary Materials).

2.2. Modelling topsoil lifespans and lateral nutrient fluxes

Topsoil lifespan is defined here as the time for the top 20 cm of soil to be physically lost from a grid cell due to water erosion. Topsoil lifespan is calculated in a similar way to Evans et al. (2020) by dividing the mass of topsoil at 0–20 cm depth, estimated from a DSM of topsoil bulk density for the same depth interval, by the erosion rate (see Text S3; Supplementary Materials). However, we have not considered rates of soil formation or accumulation via deposition as this information is unavailable.

For this study, lateral nutrient fluxes were defined specifically as soil-associated nutrients that are lost from a grid cell via soil erosion. Lateral nutrient fluxes were calculated by multiplying maps of topsoil nutrient concentrations by gross soil erosion rates (see Text S3; Supplementary Materials). As RUSLE does not calculate sediment transport or deposition (Renard et al., 1997), the fate of topsoil nutrients lost via erosion was not determined.

Gross soil erosion rates, topsoil lifespans and lateral nutrient fluxes were modelled under present-day land cover and potential natural vegetation. Elevated soil erosion, lifespan and nutrient flux rates were calculated by simply subtracting results for the natural vegetation scenario from the predictions under present-day conditions.

Given its geography, Kenya is likely to have high spatial variations in soil erosion rates. For instance, much of the north and east of the country is characterised as arid steppe or arid desert, flat (0–7 % slopes throughout),

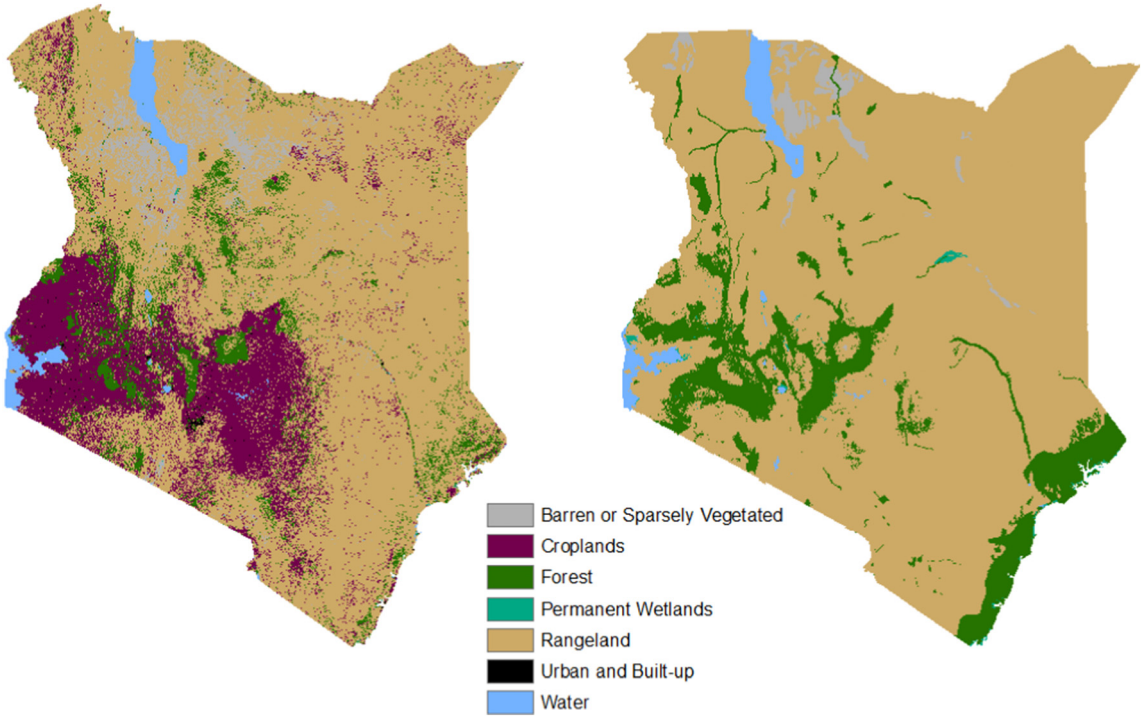

Fig. 1. Distributions of aggregated land cover classes (see Text S1; Supplementary Materials) under (left) the present-day scenario representing current land cover conditions and (right) the potential natural vegetation (PNV) scenario with no human activity (no croplands or urban and built-up areas). Rangeland includes savannah, shrubland and grassland, which are grouped together here as they have the same ranges of RUSLE C-factor coefficients. (The PNV map does not cover Ilemi in the northwest, where Kenya borders South Sudan. On the other hand, the Kenya shapefile, from the 1:10 m Cultural Vectors dataset of Natural Earth, which was used to clip the data layers from iSDA soil, does include this area. Therefore, there is a small discrepancy in borders between the two land cover scenario maps, including the soil erosion modelling results.)

and dominated by rangeland. In contrast, the western half of the country is dominated by steep terrain, high rainfall and most of Kenya's agriculture, with croplands located on steep hillsides as well as in valley bottoms. As such, it is useful to partition Kenya into different zones characterised by higher order interactions among environmental controls. Here, we applied Classification and Regression Tree (CART) modelling to partition zones representing unique interactions among controls on lateral nutrient fluxes. CART modelling offers two key advantages: (1) the relative contributions of each variable to the overall pattern of lateral nutrient fluxes across Kenya can be quantified; (2) a decision tree is produced that allows an area to be split into zones based on specified thresholds in factors such as the RUSLE LS-factor. Further details on how CART modelling was implemented can be found in Text S2 (Supplementary Materials).

2.3. Modelling of agricultural support practices

Hitherto, we have assumed that agricultural support practices do not occur, equivalent to a RUSLE P-factor of 1. This is not to say that agricultural support practices do not occur in Kenya. Indeed, as many as 80 % of farms in the Upper Tana river basin alone have adopted interventions such as establishing "*fanya juu*" (throw the soil upwards in Kiswahili) terraces, conservation tillage and intercropping (Muriuki and Macharia, 2011). However, there are no spatially explicit data on agricultural support practices for Kenya. Notwithstanding, it is still possible to test hypothetical scenarios of different interventions to conserve soil with the use of available RUSLE P-factor coefficients.

Table S1 (Supplementary Materials) displays published P-factor coefficients for various support practices including tillage, terracing, contouring and strip-contouring, that are applicable to the humid tropics (David, 1988), where most Kenyan croplands occur. These coefficients were used to create P-factor maps for croplands for every combination of support practice listed (n = 16). Details on the calculation of P-factor are in Text S1 (Supplementary Materials).

3. Results

3.1. Predicted erosion rates, topsoil lifespans and lateral nutrient fluxes

RUSLE factor maps are displayed in the Supplementary Materials, including the R-factor (Fig. S2), K-factor (Fig. S3), LS-factor (Fig. S4) and C-factor maps for each land cover scenario (Fig. S5). On average, predicted soil erosion rates by RUSLE across Kenya equal 5.5 t ha^{-1} yr^{-1}. Extrapolating this value across Kenya's ~ 58 Mha of land area results in an estimated 320 Mt of topsoil lost per year. Extrapolating average predicted lateral nutrient flux rates yields 8.8 Mt, 315 Kt and 110 Kt of SOC, N and P lost every year, respectively. Predicted erosion rates under present-day land cover are highest in the western half of Kenya, particularly near Lake Victoria and the central plateau near Mt. Kenya (Fig. 2a). Similar patterns occur under potential natural vegetation, albeit high erosion rates are less extensive than under present-day land cover and appear to cluster on steep slopes without dense forest cover (Fig. 2b). As a result, much of the west of Kenya shows substantially elevated erosion rates, with large areas exhibiting estimated erosion rates at least 5 t ha^{-1} yr^{-1} greater under present-day land cover than under natural vegetation (Fig. 2c). Some steep slopes are currently cultivated for crops. This, combined with high rainfall erosivity, and soil erodibility produce very high elevated erosion rates (>50 t ha^{-1} yr^{-1} more than under PNV). Paradoxically, some mountainous parts of Kenya indicate *lower* soil erosion rates under current land cover compared to natural vegetation conditions (Fig. 2c). This is driven by there being a lower elevation forest-shrubland boundary in the mountains according to the PNV map compared to the 2016 land cover map. We speculate that this results from misclassifications of high altitude shrubland as dense forest in the 2016 land cover map and is an artefact of comparing land cover maps that were generated at different spatial resolutions.

Reflecting these soil erosion dynamics, topsoil lifespans under current land cover are estimated to be shortest (10^1–10^2 yr timescales, mostly) in the west, with the most extreme examples showing lifespans between 1 and 10 years (Fig. 2d). Conversely, many of these same topsoils are

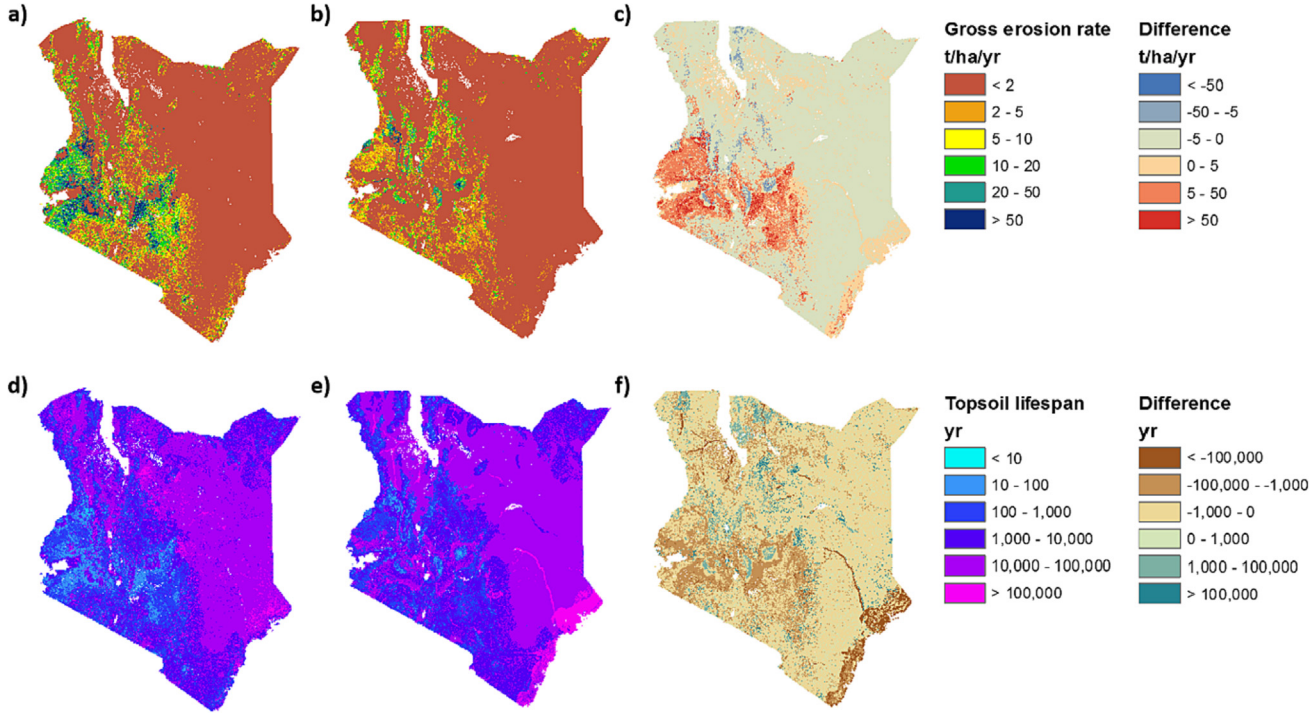

Fig. 2. Topsoil erosion rates: a) Estimated rates under present-day land cover; b) Modelled potential rates under natural vegetation; c) Differences (present-day minus natural) in gross soil erosion rates. Topsoil lifespans: d) Estimated soil lifespans under present-day land cover; e) Modelled potential soil lifespans under natural vegetation; f) Differences (present-day minus natural) in topsoil lifespans. Because (c) and (f) represent differences between present-day and natural vegetation conditions, negative values indicate where a value is larger under natural vegetation conditions and positive values indicate where it is larger under present-day land cover.

estimated to have lifespans of 10^3–10^5 years (Fig. 2e). The map of topsoil lifespan differences (Fig. 2f) illustrates the disparities between land cover scenarios. However, in some of the mountains and parts of the north, where the PNV map suggests a greater extent of barren land than present-day land cover, topsoil lifespans are estimated to be 10^3–10^5 years *shorter* under potential natural vegetation.

Lateral nutrient flux estimates also reflect soil erosion dynamics under the two land cover scenarios. Over most of Kenya, estimated lateral SOC fluxes are below 0.5 t ha^{-1} yr^{-1}, with larger rates >2.5 t ha^{-1} yr^{-1} occurring in regions with the highest estimated soil erosion rates and topsoil SOC concentrations (Fig. S6; Supplementary Materials). Similar patterns occur for lateral N fluxes (Fig. S7; Supplementary Materials), although in the case of lateral P fluxes, the total P concentration of topsoil does not appear to coincide with high flux rates (Fig. S8; Supplementary Materials). Like for soil erosion and topsoil lifespan, the differences in SOC, N and P flux rates between present land cover and potential natural vegetation conditions are greatest where croplands occur under present-day land cover.

RUSLE model results were evaluated against observed soil erosion rates at four primary sites across western Kenya: Kalalu, Matanya, Kabete and the croplands of Kericho County (see Table S2; Supplementary Materials for the coordinates of each site). Previous studies suggest that RUSLE model predictions can be considered acceptable when the prediction errors do not exceed a factor of 2 or 3 (Bagarello et al., 2012; Borrelli et al., 2017). Our predicted soil loss rates at Kalalu (27.3 cf. the observed 12.4 t ha^{-1} yr^{-1}), Matanya (5.5 cf. the observed 4.1 t ha^{-1} yr^{-1}) and the croplands of Kericho County (53.4 cf. the observed 97.8 t ha^{-1} yr^{-1}) can thus be considered acceptable. However, RUSLE-predicted soil loss rates (90.5 t ha^{-1} yr^{-1}) fell far short of observed (346.6 t ha^{-1} yr^{-1}) rates at Kabete (Fig. S9; Supplementary Materials). These results are in keeping with the prevailing observation that RUSLE over-estimates low and under estimates high soil erosion rates (Kinnell, 2005). Evans et al. (2020) synthesised global data on soil erosion and formation rates and used these data to estimate topsoil (in that study, the top 30 cm) lifespans. After calculating topsoil lifespans here (the top 20 cm), it was found that all estimated values were within the same order of magnitude as those estimated by Evans et al. (2020) across Kalalu, Matanya, Kabete and croplands in Kericho County (Fig. S10; Supplementary Materials).

Soil erosion modelling presented here shows a small proportion of very large predicted rates across Kenya. The largest soil erosion rate category visualised in our RUSLE maps is >50 t ha^{-1} yr^{-1}, which includes 1–5 % of all grid cells across Kenya (Fig. S11; Supplementary Materials). The top 0.01 % of all modelled cells show predicted soil erosion rates >100 t ha^{-1} yr^{-1}, with the most extreme examples exceeding 1000 t ha^{-1} yr^{-1} (Fig. S11; Supplementary Materials). Compared with the top 1 %, grid cells displaying the top 0.01 % of predicted soil erosion rates show much larger C, K, LS and R-factor values on average (Fig. S12; Supplementary Materials). It is highly unlikely that such enormous soil erosion rates would occur through rill and sheet erosion alone (the processes that RUSLE is concerned with explicitly). Therefore, the most we might be able to interpret from this is that these are simply soil erosion hotspots according to the RUSLE model projections. Elsewhere, it is likely that other erosion mechanisms such as gullying may become dominant but are not captured in the RUSLE modelling, resulting in model estimates that are likely too low. This remains a key research challenge.

Our CART modelling revealed the relative importance of each RUSLE factor on predicted soil erosion rates. LS and C-factor were revealed to drive >75 % of soil erosion across Kenya under present-day land cover, representing 41 % and 36 % importance, respectively (Table S3; Supplementary Materials). Under natural vegetation, C-factor was most important (40 %) followed by LS-factor (38 %), perhaps reflecting the effectiveness of greater forest cover in supressing soil erosion under this scenario. R-factor contributed 21–22 % and K-factor 1 % importance under both vegetation cover scenarios (Table S3; Supplementary Materials).

3.2. Regional controls and process rates within Kenya

The assessment of nutrient fluxes is particularly important due to the potential off-site environmental risks that these fluxes pose, especially to river and lake water quality. CART modelling of the controls on lateral nutrient fluxes was used to partition seven zones. There are different ways in which RUSLE factors and topsoil nutrient concentrations interact to control estimated lateral fluxes of SOC compared with total N and total P. Therefore, the seven zones are defined differently for each nutrient as Table 1 shows. For each nutrient, the seven zones summarise key environmental properties including dominant land cover (Table 1), average soil erodibility, rainfall erosivity, slope length-steepness factor, and disparities in gross erosion rates, topsoil lifespans and lateral nutrient fluxes between current land cover and potential natural vegetation conditions (Figs. 3, 4 & 5).

Estimated lateral SOC fluxes across Kenya are controlled primarily by the LS- and C-factors (35 & 31 %, respectively), followed by R-factor (25 %) with SOC concentration (8 %) and K-factor (1 %) contributing very little (Table S4 & Fig. S13; Supplementary Materials). Most of Kenya falls within Zone 1 (Fig. 3a), characterised by low lateral SOC flux estimates (0.01 t ha^{-1} yr^{-1} on average) as a result of low LS and R values (Table 1). Zone 2 occurs in the west, where R is higher, and Zone 3 is most common on steeper slopes with rangeland vegetation. Zones 1–3 represent the regions with the lowest mean estimated erosion and lateral SOC flux debts. However, the large estimated mean topsoil lifespan disparity (12,354 yrs) in Zone 2 probably reflects the much higher proportion of forest cover under the PNV scenario (Fig. 3b, c & d). Zones 5–7 represent regions where estimated soil erosion and lateral SOC flux disparities are very large on average (95.9–356.4 t ha^{-1} yr^{-1} of soil loss; 2.9–11.9 t ha^{-1} yr^{-1} of SOC loss). Zone 7 contains some of the highest K, LS and R values in all of Kenya (Fig. 3e, f & g) and is covered mostly by cropland under present-day land-use (Table 1). Here, the estimated soil erosion differences are >300 t ha^{-1} yr^{-1} on average. Zone 4 is characterised by intermediate mean RUSLE factor values.

Estimated lateral N fluxes are controlled chiefly by LS-factor (37 %) and total N concentration in topsoil (25 %). This is followed by R (20 %) and C (18 %), with K-factor (1 %) being least important (Table S4 & Fig. S14; Supplementary Materials). Like SOC, for controls on lateral N fluxes, most of Kenya is mapped as Zone 1 (Fig. 4a). Unlike SOC, however, Zone 1 is defined here as parts of the country where estimated total N concentration is <1 g kg^{-1} and the terrain is flat (Table 1). Zones 2–4 are characterised by relatively small estimated average disparities of erosion rates, lateral N fluxes and topsoil lifespans (Fig. 4b, c & d). Zone 4 is predominantly forest under both land cover scenarios, but also includes some of the mountainous areas that have less forest cover under the PNV scenario. Zone 5 exhibits the largest mean estimated topsoil lifespan disparities (28,888 yrs) in Kenya, which likely reflects the differences in predominant land cover under the two scenarios (cropland under current land cover and forest under the PNV scenario). Zones 6 and 7 are marked by the highest estimated average erosion and lateral N flux disparities (112.8–316.6 t ha^{-1} yr^{-1} of soil loss: 0.1–0.4 t ha^{-1} yr^{-1} of N loss). This is due to the combination of land cover differences between the two scenarios (cropland versus forest; see Table 1) and the high mean LS, K and R values in Zone 7 (Fig. 4e, f & g).

Estimated lateral P fluxes are controlled in a similar fashion to lateral SOC fluxes. LS and C are the main drivers (42 % & 35 %, respectively), then R (19 %), with total P content (4 %) and K (0 %) contributing very little overall (Table S4 & Fig. S15; Supplementary Materials). Again, much of Kenya falls within Zone 1 (Fig. 5a), characterised by relatively little estimated soil erosion and land cover differences between the two land cover scenarios (Fig. 5b). Large lifespan disparities (38,043 yrs) in Zone 2 (Fig. 5c) reflect the predominance of croplands under present-day land cover compared with much greater extents of rangelands under the PNV scenario (Table 1). In contrast, Zones 4 and 5 reflect higher proportions of forest cover under current land cover (Fig. 5b, c & d). Zones 6 and 7 exhibit the greatest modelled erosion and lateral P flux disparities (0.02–0.09 t ha^{-1} yr^{-1}), which can be explained by the interactions of

Table 1
The modal land cover category in each nutrient flux zone under the present-day land cover and PNV scenarios according to our modelling. The Zone column details the delineation of each zone (**N** = Total N flux rate [t ha^{-1} yr^{-1}], **LS** = slope length and steepness [unitless], **R** = rainfall-runoff erosivity [MJ mm ha^{-1} h^{-1} yr^{-1}] and **C** = cover-management [unitless]).

Nutrient	Zone	Area (ha)	Present-day land cover	Potential natural vegetation
SOC	1) **LS** < 1.4 & **R** < 3131	45,234,610	Rangeland	Rangeland
	2) **LS** < 1.4 & **R** ≥ 3131	4,166,104	Croplands	Rangeland
	3) **LS** ≥ 1.4 & **C** < 0.22	4,396,355	Forest	Rangeland
	4) 1.4 ≤ **LS** < 3.3, **C** ≥ 0.22 & **R** < 6350	1,322,823	Croplands	Forest
	5) **LS** ≥ 3.3, **C** ≥ 0.22 & **R** < 6350	689,226	Croplands	Forest
	6) 1.4 ≤ **LS** < 4.5, **C** ≥ 0.22 & **R** ≥ 6350	42,736	Croplands	Forest
	7) **LS** ≥ 4.5, **C** ≥ 0.22 & **R** ≥ 6350	28,896	Croplands	Forest
Total N	1) **N** < 1 & **LS** < 1.1	46,749,127	Rangeland	Rangeland
	2) **N** < 1, **LS** ≥ 1.1 & **C** < 0.22	3,282,528	Rangeland	Rangeland
	3) **N** < 1, **LS** ≥ 1.1 & **C** ≥ 0.22	1,219,221	Croplands	Rangeland
	4) **N** ≥ 1 & **C** < 0.22	2,217,953	Forest	Forest
	5) **N** ≥ 1, **C** ≥ 0.22 & **LS** < 3	1,889,122	Croplands	Forest
	6) **N** ≥ 1, **C** ≥ 0.22, **LS** ≥ 3 & **R** < 6753	484,350	Croplands	Forest
	7) **N** ≥ 1, **C** ≥ 0.22, **LS** ≥ 3 & **R** ≥ 6753	38,449	Croplands	Forest
Total P	1) **LS** < 1.4 & **C** < 0.22	38,901,169	Rangeland	Rangeland
	2) **LS** < 0.52 & **C** ≥ 0.22	7,082,051	Croplands	Rangeland
	3) 1.4 ≤ **LS** < 1.4 & **C** ≥ 0.22	3,417,493	Croplands	Rangeland
	4) **LS** ≥ 1.4 & **C** < 0.041	1,711,159	Forest	Forest
	5) **LS** ≥ 1.4 & 0.041 ≤ **C** < 0.22	2,685,196	Rangeland	Rangeland
	6) **LS** ≥ 1.4 & **C** ≥ 0.22 & **R** < 6551	2,021,606	Croplands	Forest
	7) **LS** ≥ 1.4 & **C** ≥ 0.22 & **R** ≥ 6551	62,075	Croplands	Forest

large K, LS and R RUSLE factor values (Fig. 5e, f & g). Croplands dominate Zones 6 and 7 under present-day land cover; in contrast forests cover these same zones under the PNV scenario (Table 1). Therefore, there will be large differences in the RUSLE C-factor as well that contribute to large modelled disparities here.

3.3. Effects of agricultural support practices

Under most combinations of agricultural support practices, our modelling indicates that erosion rates are reduced to levels comparable to converting croplands to PNV (Fig. 6). Zoned and mulch tillage-based

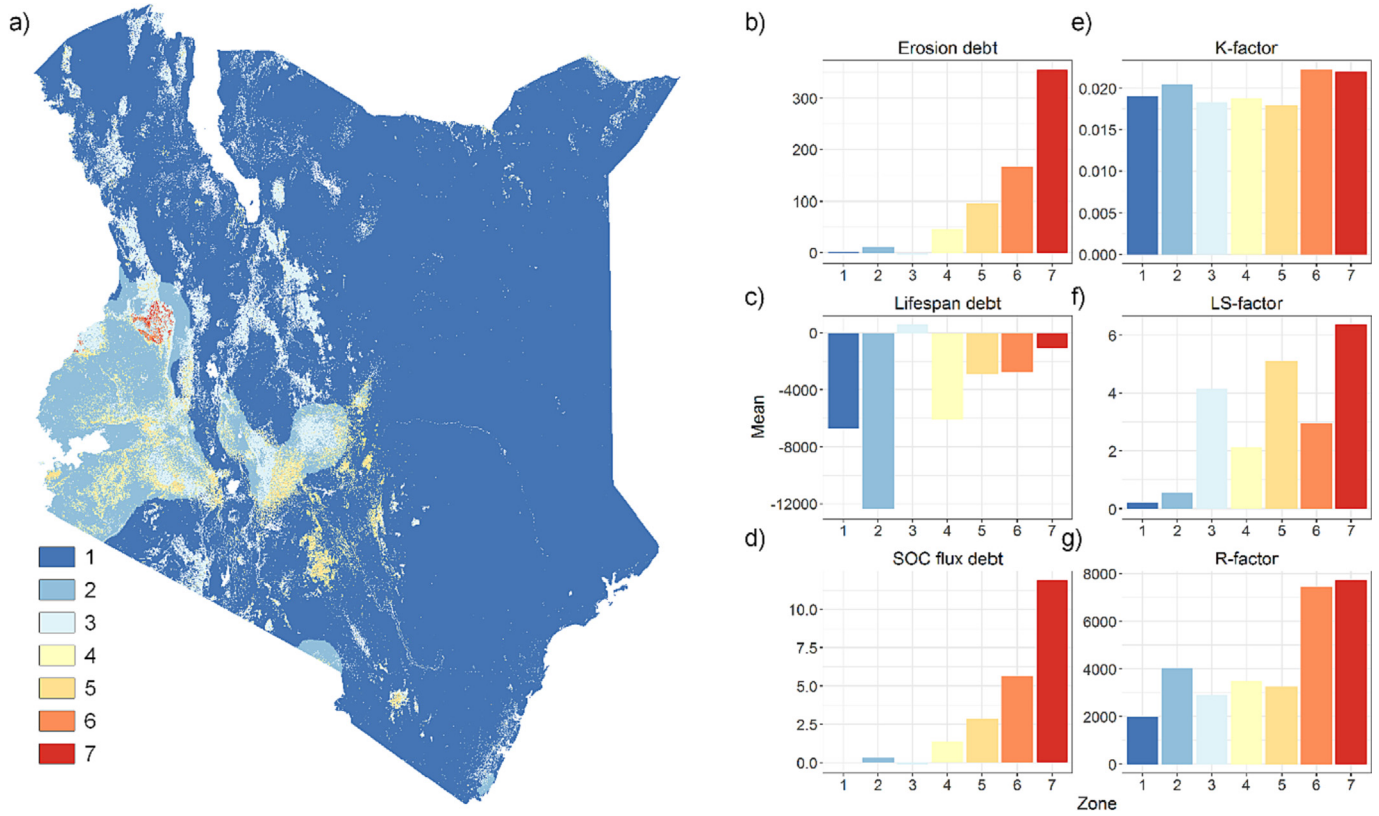

Fig. 3. a) Seven distinct zones characterised by controls, described in Table 1, on estimated rates of lateral SOC fluxes under present-day land cover. The mean b) erosion rate (t ha^{-1} yr^{-1}), c) topsoil lifespan (yr) and d) SOC flux rate disparities (t ha^{-1} yr^{-1}) (present-day minus PNV scenario equals "debt") in each zone. The mean of the RUSLE factors, e) K (t ha h MJ^{-1} ha^{-1} mm^{-1}), f) R (MJ mm ha^{-1} h^{-1} yr^{-1}) and g) LS (dimensionless) within each zone.

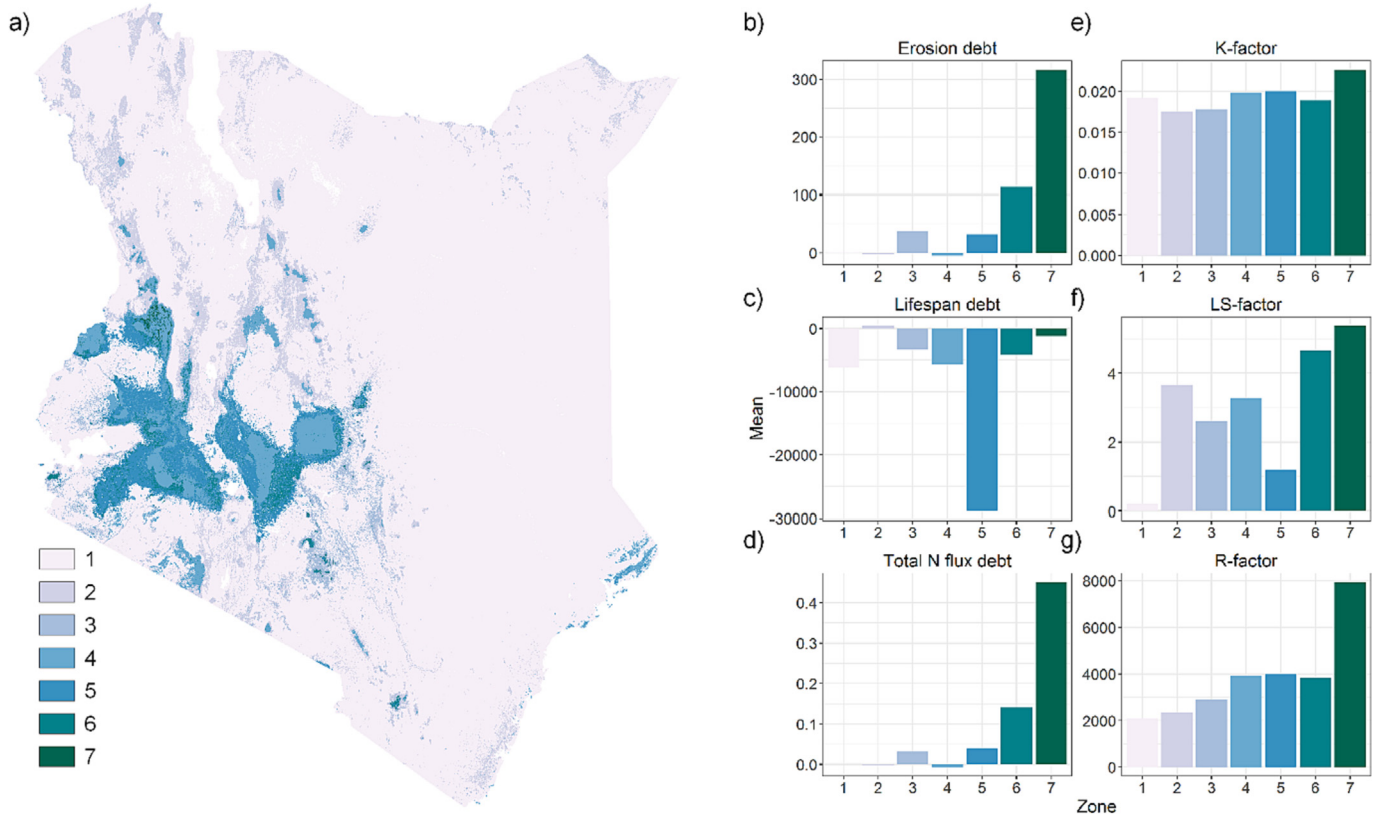

Fig. 4. a) Seven distinct zones characterised by controls, described in Table 1, on rates of lateral N fluxes under present-day land cover. The mean b) erosion rate (t ha^{-1} yr^{-1}), c) topsoil lifespan (yr) and d) Total N flux rate disparities (t ha^{-1} yr^{-1}) (present-day minus PNV scenario equals "debt") in each zone. The mean of the RUSLE factors, e) K (t ha h MJ^{-1} ha^{-1} mm^{-1}), f) R (MJ mm ha^{-1} h^{-1} yr^{-1}) and g) LS (dimensionless) within each zone.

practices induce the steepest reductions in erosion rates, especially when combined with either of the terracing interventions. The most effective intervention – combining bench terracing with zoned tillage – reduces modelled soil loss rates by at least 75 % on all croplands, and by >95 % in most cases (Fig. 7). Here, the median reduction in modelled soil loss rates is about 9.7 t ha^{-1} yr^{-1}, and in the top 5 % of cases, estimated erosion rates are reduced by at least a factor of 9. Even the least effective intervention – combining conventional tillage with contouring – reduces soil erosion rates by 40–50 % across most croplands (Fig. 7), and by an overall median value of about 4.4 t ha^{-1} yr^{-1}. To put this into perspective, taking the median bulk density (1.32 g cm^3) and soil formation rates (0.035 mm yr^{-1}) reported for Kenya (Liniger, 1992), an erosion rate reduction of 4.4 t ha^{-1} yr^{-1} (equivalent to 0.333 mm yr^{-1}) is >7 times the estimated tolerable soil loss of 0.046 mm yr^{-1} (see "Liniger" in Supplementary Table 2 of Evans et al., 2020). Although not shown here, it should be safe to assume that these interventions would be similarly powerful in reducing lateral fluxes of SOC, N and P, and for enhancing topsoil lifespans.

4. Discussion

4.1. Erosion implications and mitigation in Kenya

Globally, soil erosion rates from conventionally tilled croplands outpace soil formation rates by at least an order of magnitude (Montgomery, 2007). Consequently, many soils are undergoing rapid rates of thinning and their profiles have short lifespans. As soil thickness controls soil functioning, including water retention, and nutrient storage capacities, thinning is a major threat to long-term soil sustainability (Power et al., 1981). These links between topsoil erosion, lifespans and nutrient storage underpin our integrated modelling approach of erosion and its effects on topsoil properties which is discussed below.

Recently, it was revealed that ~93 % of conventionally managed soils were thinning and ~16 % had short lifespans <100 years (Evans et al., 2020). In contrast, ~7 % of conservation plots had short lifespans <100 years, with ~39 % having long lifespans >10,000 years; this demonstrates the role that land-use management plays in conserving soil (Evans et al., 2020). Our modelling suggests that 3.1 Mha, 86 % of which are croplands, in Kenya are estimated to have short topsoil lifespans <100 years. This suggests that croplands are a significant hotspot of soil thinning and ameliorating thinning in these areas will be key to increasing topsoil lifespans.

Like soil thickness, soil organic matter (SOM) plays a fundamental role in soil structure and functioning. SOM consists mainly of SOC and contains large amounts of N and P, with a change in any one of these nutrients directly influencing the other two. For example, enhanced mineralisation of SOC associated with soil erosion will cause a relative increase in the more biologically accessible dissolved forms of N and P (Quinton et al., 2010). Together with high erosion rates and soils that are generally nutrient-poor, SOC-N-P feedbacks may exacerbate land degradation problems across Kenya, especially where vegetation cover is reduced (Hartemink et al., 2008; Smaling et al., 2015) and erosion-associated nutrient losses outstrip fertiliser inputs (Mulinge et al., 2016; Quinton et al., 2010). Accelerating erosion here may induce land cover change, which itself will perturb SOC, N and P cycling directly and, indirectly, by contributing to climate change through further losses of C to the atmosphere in the form of greenhouse gases (Bakker et al., 2005; Feddema et al., 2005; Quinton et al., 2010). Our own modelling provides for the first time, maps of SOC, N and P fluxes associated with soil erosion at high spatial resolution (30 m). These maps could be used to guide future monitoring and interventions to conserve nutrients in Kenya's soils, or as data inputs for further modelling (e.g. of C, N and P exchanges between soil, vegetation, freshwater bodies and the atmosphere).

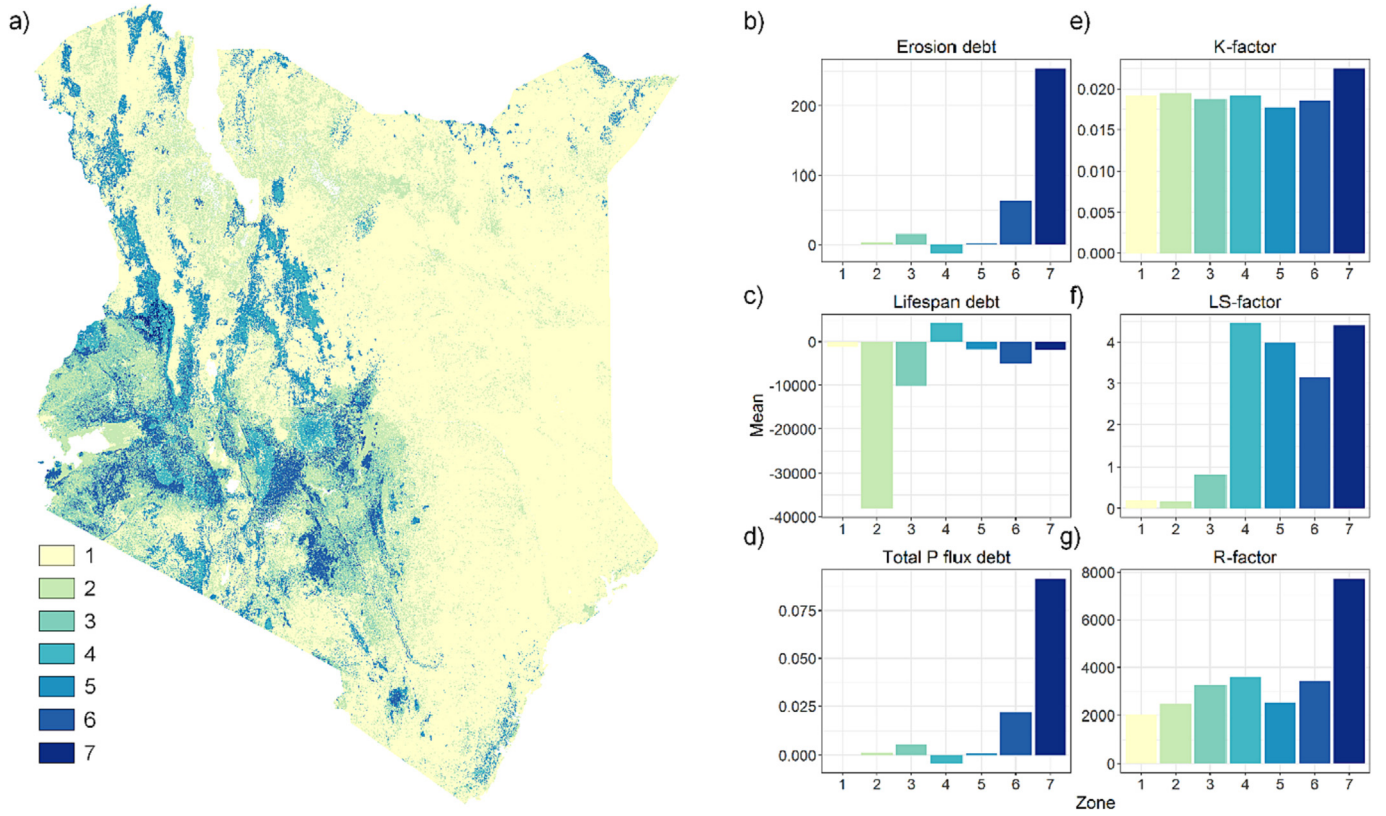

Fig. 5. a) Seven distinct zones characterised by controls (see Table 1), on rates of lateral P fluxes under present-day conditions. Mean b) erosion rate (t ha^{-1} yr^{-1}), c) topsoil lifespan (yr) and d) Total P flux rate disparities (t ha^{-1} yr^{-1}) (present-day minus PNV scenario equals "debt") for each zone. The mean of the RUSLE factors, e) K (t ha h MJ^{-1} ha^{-1} mm^{-1}), f) R (MJ mm ha^{-1} h^{-1} yr^{-1}) and g) LS (dimensionless) within each zone.

In Kenya, the impacts of nutrient fluxes to aquatic ecosystems have been well documented, especially in the case of the Winam Gulf of Lake Victoria (May et al., 2022). Blooms of the invasive water hyacinth (*Eichhornia crassipes*), which threaten fishing activities and block water pumps, have intensified in recent years as suspended sediment, N and P loads from contributing river basins have increased (Nyawacha et al., 2021). Locally, high sediment and P loads are driven by agricultural runoff, and the erosion of riverbanks and P-rich carbonatite rocks (Guya, 2019). Our results appear to reflect this, which show the upper reaches of rivers draining into Winam Gulf such as the Nyando and Sondu-Miriu basins are classed as zones 5 to 7 in Figs. 3-5 (areas contributing the largest nutrient flux rates). Given the climate of Kenya, the fluxes of sediments and associated nutrients from rivers into Lake Victoria are likely to be greatest during the rainy seasons (March–May and August–October), which Humphrey et al. (2022) demonstrated using the RUSLE model at monthly resolution.

Alewell et al. (2020) highlighted that Africa has some of the highest soil P depletion rates in the world, driven by the challenges of fertiliser affordability and exacerbated by high soil erosion rates. Indeed, although fertiliser use has increased on average across Kenya from 82 kg ha^{-1} in 1992 to 100 kg ha^{-1} in 2013, this remains far below the recommended levels to sustain high crop yields long-term (Jena et al., 2021). Together, high erosion rates and insufficient fertiliser use are likely driving stagnant yields on Kenyan croplands (Fig. S16; Supplementary Materials). Our own modelling shows that elevated soil erosion rates are driving high rates of SOC, N and P losses across Kenya, especially on croplands. The comparisons of predicted erosion and nutrient flux rates under present land cover with natural baseline conditions (mapped in Fig. 2 and Figs. S6-S8; Supplementary Materials) may help landowners and policy makers to intervene to reduce future losses of soil and nutrients. For example, relatively flat terrain (slopes of 0–7 %) may require extra tree planting and use of cover crops to reduce bare soil exposure; steeper terrain meanwhile may require the construction of terraces to break up long and steep slopes that could convey large volumes of eroded soil very rapidly into water courses.

Mitigating elevated soil erosion and nutrient flux rates requires an understanding of how these rates are being driven spatially. The CART modelling approach we applied to estimate regional drivers of soil erosion across Kenya follows earlier work on global scale modelling by Borrelli et al. (2017). In our study, the CART modelling revealed that slope length-steepness and land cover account for >75 % of the relative contribution to soil erosion rates across Kenya, and this is broadly commensurate with the published global scale analysis (Borrelli et al., 2017). This is unsurprising given the steep valley topography found in much of western Kenya. While rainfall erosivity can be important (especially near Lake Victoria where annual rainfall rate is highest), slope morphology is very important for carrying away any soil particles detached by rain splash. CART modelling could be applied at smaller scales such as river catchments or individual fields. Within these alternative contexts, factors such as soil erodibility or the relationship between rainfall erosivity and slope might be found to be most important. If so, CART modelling would reveal very different process interactions and necessitate using alternative intervention strategies like cover crops to reduce soil losses. However, our findings that topography and land cover drive most of the erosion rates are also commensurate with studies at plot (Benkobi et al., 1994) and catchment (Estrada-Carmona et al., 2017) scales. Thus, the interventions that we would recommend based on our national-scale analysis will likely apply just as effectively at smaller scales such as individual river catchments. Similar statistical modelling could also be applied to other drivers of soil loss, such as wind erosion. This would provide a more complete assessment of the main controls on soil erosion dynamics which could usefully guide the design of interventions to mitigate elevated soil loss rates.

Given our findings that, apart from on forested lands, the combination of slope length and steepness is the key factor driving modelled soil loss rates under different land cover types, interventions aimed at modifying

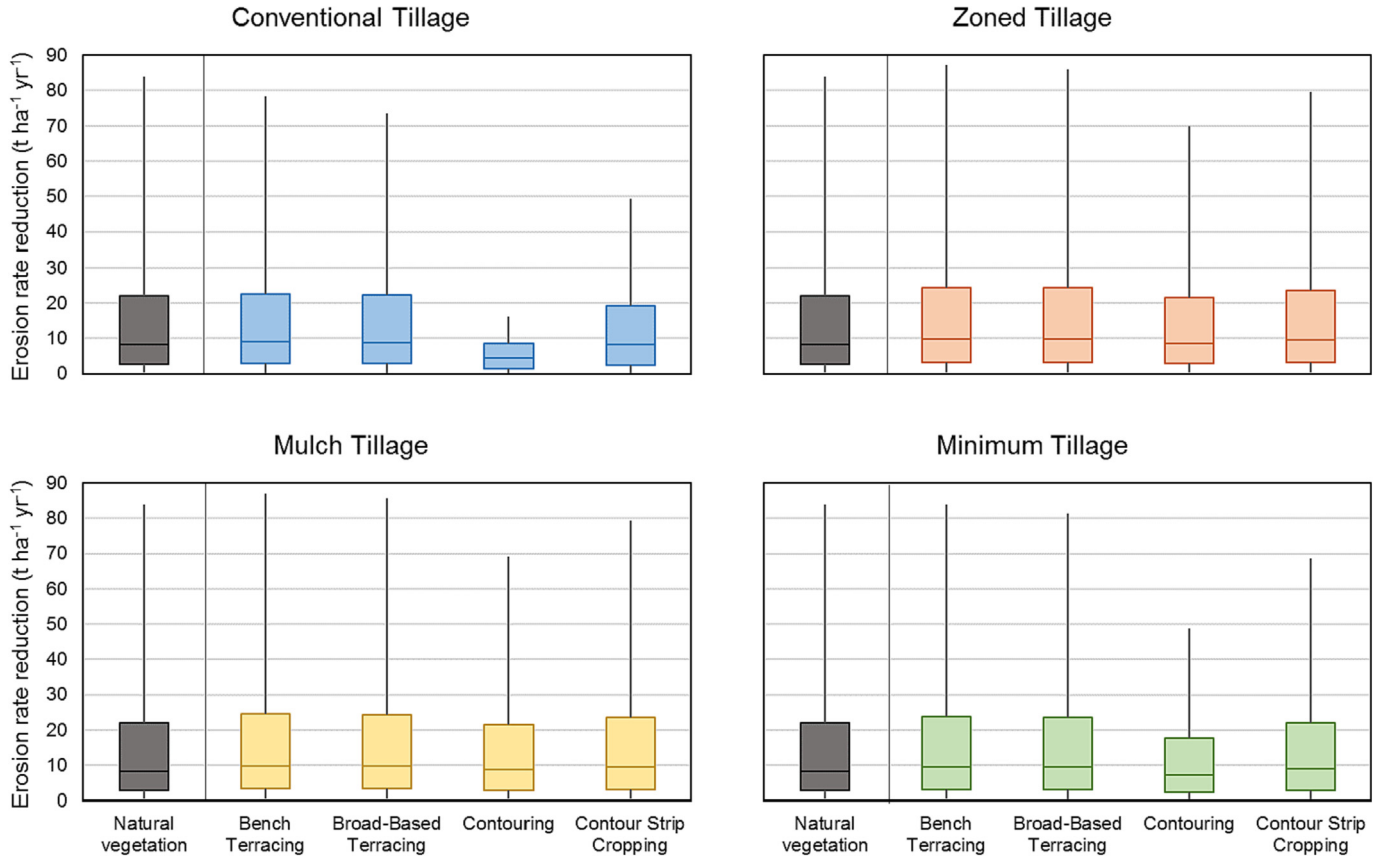

Fig. 6. Erosion rate reductions in croplands under various agricultural support practices compared with converting back to natural vegetation cover. Whiskers on the boxplots extend to the 5th and 95th percentiles.

slopes and surface runoff pathways should be a priority for preventing soil loss. The effects of many such interventions can be modelled by RUSLE via the support practices P-factor. The scenarios tested here focus on combinations of different tillage practices with measures including terracing, contouring and contour strip-cropping for two reasons. First, these interventions are applied widely across Kenya; second, minimum and no-till practices are known to generally reduce surface runoff compared to conventional tillage (e.g. Strauss et al., 2003), while terracing breaks up the slope to promote infiltration and reduce surface runoff (Arnáez et al., 2015). Introducing either bench or broad-based terracing was found to reduce modelled soil erosion rates on croplands by a similar extent to converting these lands to natural vegetation cover (Fig. 6). Similar effects of terracing were measured in Rwanda with up to 93 % reductions in soil loss rates recorded (Rutebuka et al., 2021). Contouring on Ethiopian hillslopes meanwhile yields similar P-factor coefficients (0.57–0.9) to the ones we tested (0.5–0.95) in Kenya (Taye et al., 2017). Not only do terracing and reduced tillage practices reduce soil erosion, they improve soil fertility by limiting nutrient losses, and promoting SOM accumulation and formation of stable aggregates (e.g. Kagabo et al., 2013; Rutebuka et al., 2021). While it would be possible to estimate nutrient loss rates under these interventions, we could not verify if introducing terraces and reduced tillage promotes additional SOC, N and P accumulation. This is not possible to test with RUSLE, but it would be a useful subject for a future modelling study.

4.2. Uncertainties, limitations and future research

The RUSLE model has been applied to Kenya several times in the past, including at national scale (e.g. Kassam et al., 1991; Watene et al., 2021), and as part of global scale modelling (Borrelli et al., 2017). Where national scale predictions exist, estimated long-term soil loss rates are no higher than 5 t ha^{-1} yr^{-1} across most of the country, particularly in the flat (0–7 % slope), arid and uncultivated northern and eastern regions of Kenya (Borrelli et al., 2017; Watene et al., 2021). This is replicated by our own modelling of predicted soil erosion rates under present-day land cover (Fig. 2a). Projected soil erosion hotspots, where modelled rates exceed 20 t ha^{-1} yr^{-1}, occur throughout much of western Kenya (see Supplementary Fig. 2 in Borrelli et al., 2017). Again, our modelling reflects this (Fig. 2a), including under the PNV scenario (Fig. 2b), likely due to the limited protection from erosion conferred by rangeland vegetation on very steep slopes.

Like this study, Watene et al. (2021) produced national-scale predictions of soil erosion rates across Kenya at 30 m grid resolution using the RUSLE model. They also summarised their results by regions defined by various physiographical and administrative units. Comparing our erosion rate predictions shows close similarities between the results in this work and those of Watene et al. (2021) by region (Fig. S17; Supplementary Materials). For 37 out of 43 (~86 %) regions, the difference between our two studies was <50 % (Fig. S17; Supplementary Materials). We would expect to see some discrepancies in modelled soil loss rates, considering that the input datasets and calculations for the R, K, C and LS factors differ between the two studies. Nevertheless, there are strong agreements overall between model predictions for the spatial distribution and magnitudes of soil erosion rates, which we argue should support a high level of confidence in our own predictions.

However, several model uncertainties exist which stem from limitations in the design of RUSLE, including landscape evolution processes, such as deposition and gullying that are not captured by the modelling, and the appropriateness of applying RUSLE outside of temperate agricultural environments (see Alewell et al., 2019; Benavidez et al., 2018; Labrière et al., 2015). We detail the model limitations with respect to Kenya's environmental context and the model input layers, including the two land cover

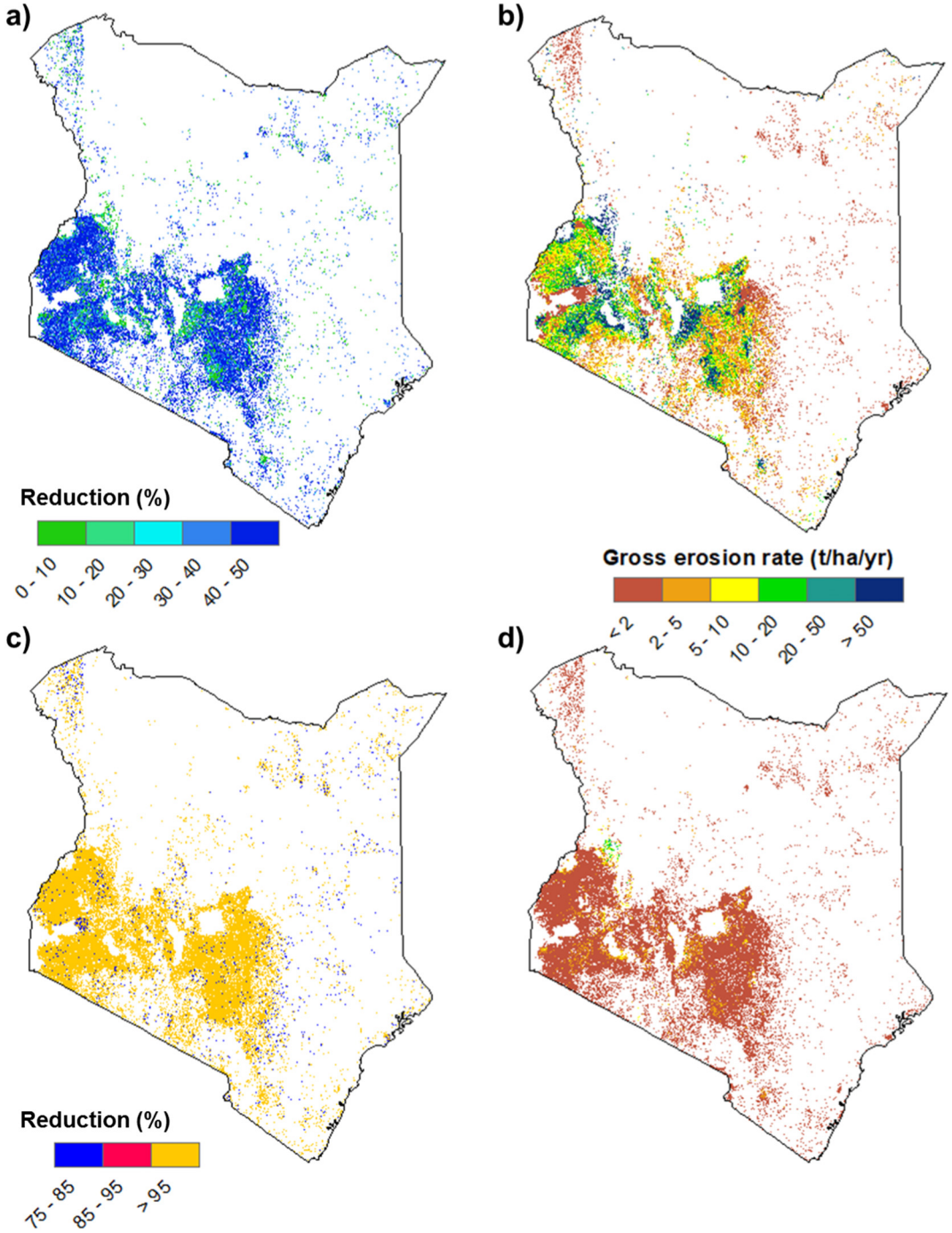

Fig. 7. Effects of the least effective (contouring with conventional tillage) and most effective (bench terracing with zoned tillage) changes in land management practices on soil erosion rates on croplands across Kenya: a) Percentage reduction in erosion rates by the **least effective** measure compared to present-day settings with no interventions; b) Gross soil erosion rates on croplands after the **least effective** intervention is introduced; c) Percentage reduction in erosion rates by the **most effective** measure compared to present-day settings with no interventions; d) Gross soil erosion rates on croplands after the **most effective** intervention is introduced.

maps, in the Supplementary Materials (Text S4). In the remainder of this discussion, we focus on limitations to coupling RUSLE-predicted soil erosion rates with topsoil lifespans and nutrient fluxes and suggest how this coupling might be improved.

The increased availability of high spatial resolution digital soil maps (DSMs) has opened new opportunities to predict soil erosion and its consequences at large scale. DSMs of physical properties make for easy estimation of soil erodibility, soil mass and thinning rates, while chemical properties can be combined with erosion rates to simulate important biogeochemical fluxes. While the proliferation of new DSMs will be helpful, the predicted values of soil properties will depend on the quality and quantity of input soil data, covariate layers such as parent material and land cover maps that control the magnitude of a soil property, and the methods used to generate the DSM such as regression kriging and machine learning. It has been shown, for instance, that DSMs of topsoil texture across Ghana differ markedly from each other (Maynard et al., 2022), with similar findings uncovered for SOC DSMs of Great Britain (Feeney et al., 2022). Uncertainties in the DSMs used for our study will affect predicted soil erodibility, lateral nutrient fluxes and topsoil lifespans. However, given the relatively minor importance of soil erodibility compared to topography and land

cover in our study, the impact of DSM uncertainties on our model results should be minimal.

The calculation of topsoil lifespans uses a simple mass balance approach based on estimating the mass of topsoil and losses in relation to erosion rates. This type of mass balance approach, which has been used to estimate the residence times of sediments deposited in upland valleys (Dietrich and Dunne, 1978) and river floodplains (Feeney et al., 2020), can provide an initial indicator of erosion severity. However, unlike Evans et al. (2020), the calculation of topsoil lifespans used here did not consider soil formation rates. There are very few estimates of soil formation rates for Kenya and these will vary as a function of the key soil formation factors: parent material, topography, organisms, climate and time (Jenny, 1941). Consequently, we cannot yet incorporate soil formation rates into our modelling. Therefore, our lifespan predictions in general are likely to be conservative estimates and suggest that all topsoils are thinning. At smaller scales, without deposition predictions, topsoils in landforms such as piedmonts probably have much longer lifespans than our modelling suggests. Conversely, the exclusion of other erosion processes, such as gullying and landslides, means lifespans may be under-estimated by significant amounts at affected locations. Enhancing our understanding of soil loss and accumulation by landform type should improve quantification of topsoil lifespans. Lastly, we assume that long-term soil erosion rates will not fluctuate over the course of a topsoil lifespan. This becomes increasingly unrealistic with longer lifespans, and if soil properties change significantly with depth, thinning rates may increase or decrease markedly (Batista et al., 2022). We have tried to control for varying erosion rates at depth by calculating lifespans for the topsoil only.

Although shown here through our modelling that support practices reduce erosion rates substantially, important caveats must be addressed. First, the range of support practices is enormous and these are not always applied individually. Second, we assume that the coefficient of one support practice is multipliable by another to estimate their combined reduction of soil erosion rates. This may not be the case and, given the multitude of different combinations, a huge amount of observational data is necessary to verify this. Third, we do not know how effective adopted practices will be in the long-term. Conservation trenches and stone bunds, for instance, are known to degrade after only a few rainy seasons due to infilling with eroded sediment from up slope (Taye et al., 2015). We also assume that interventions have been applied optimally and remain well maintained. Terraces, if installed poorly or abandoned, can worsen rather than reduce soil erosion (Deng et al., 2021). Thus, even though a support practice may be present, it does not mean that it is working at its full potential. Fourth, the quantity and exact locations of specific agricultural support practices cannot be mapped accurately yet, meaning the P-factor is seldom taken into account in modelling at large spatial scales (Fenta et al., 2020). Hence, the reader should take care to interpret our scenario modelling results as preliminary and requiring verification.

As there are relatively few available observations in Kenya of soil loss rates, nutrient fluxes and estimated topsoil lifespans, it is difficult to properly verify the accuracy of our modelling against real-world processes. Such constraints on data availability are not uncommon and in part at least, this has led some to suggest that model validation sensu stricto is impossible to attain (Oreskes, 1998; Oreskes et al., 1994). Indeed, validation issues bedevil all models of Earth surface dynamics. For example, incomplete representation of fluvial processes and scarce historical observation data have led users of the CAESAR-Lisflood landscape evolution model to adopt model *evaluation* over *validation* (Feeney et al., 2020; Meadows, 2014; Pasculli and Audisio, 2015). Evaluation has the advantage of considering model shortcomings and uncertainties in addition to comparing predictions with existing datasets. The few assessments we could make against measured erosion rates and topsoil lifespans (e.g. Figs. S9-S12 & S17; Supplementary Materials), indicate the model performed well overall. However, extremely high soil loss predictions occurred in <1 % of grid cells that are most likely unrealistic (Fig. S11; Supplementary Materials).

Notwithstanding limitations inherent in the model predictions, our results present the first approximation of the integrated dynamics of erosion, lateral nutrient fluxes and topsoil lifespans for Kenya, and demonstrate the direction and scale of change with changing patterns of land cover and management. Interpreting these results should be taken in terms of: i) the spatial distributions of high and low magnitude process rates relative to Kenya on average; ii) the effects of tested scenarios relative to one another; and iii) how the phenomena of i) and ii) might be explained by the understanding of process controls and their interactions at various scales. Further, our modelling represents a highly comprehensive assessment of the consequences of erosion on soil structure at a national scale. Future research should be directed more towards targeted long-term monitoring, as this would both improve soil loss predictions in future and facilitate the integration of other processes such as sediment transport to get a more complete assessment of soil erosion dynamics. Our results provide both a useful assessment of topsoil degradation from erosion and a proof of concept that can guide policy and innovation, and be adapted for future modelling (e.g. of additional topsoil characteristics, environmental change scenarios or degrading landscapes elsewhere).

5. Conclusion

We applied an integrated modelling approach to predict soil erosion risk, associated loss rates of SOC, N and P, and topsoil lifespans across Kenya under both current land use and PNV conditions. Our analysis revealed four key findings. First, modelled soil erosion is most severe in the west of the country where croplands, steep slopes and high annual rainfall predominate. Second, accelerated erosion rates drive increased modelled lateral fluxes of SOC, N and P, and topsoil lifespans decline by multiple orders of magnitude. Third, topography and land cover are the main drivers of modelled erosion rates everywhere apart from in forested areas. This is just as true for the PNV scenario as it is for present-day land cover, illustrating that large soil losses can occur even under natural baseline conditions. Fourth, incorporating into croplands agricultural support practices that decrease surface runoff by interrupting slope profiles are just as effective at reducing modelled soil erosion rates as converting these lands to natural vegetation cover. We can therefore accept both of our hypotheses: that present-day soil erosion rates are elevated due to current land cover patterns (particularly on croplands); and applying agricultural support practices (specifically terracing and reduced tillage) can reduce soil erosion rates back to natural baseline levels.

While our modelling successfully demonstrates how elevated soil erosion rates can be ameliorated, additional long-term monitoring of an extensive number of cropland sites with agricultural support practices in place is required to verify our predictions. The methodology we used is applicable to different contexts, including in other biomes, and could be expanded to capture erosion from wind, gullying and mass movements. Future research should also focus on other land degradation pathways besides soil erosion, notably above and below ground carbon stocks and forest cover. This would give a more complete assessment of land degradation and spur innovation to deliver long-term sustainable land use under global environmental change.

CRediT authorship contribution statement

Christopher J. Feeney: Conceptualisation, Methodology, Investigation, Formal Analysis, Data Curation, Writing- Original draft preparation. David A. Robinson: Conceptualisation, Supervision, Writing - Review & Editing. Amy R.C. Thomas: Supervision, Writing - Review & Editing, Pasquale Borrelli: Methodology, Writing - Review & Editing. David M. Cooper: Writing - Review & Editing. Linda May: Project Administration, Writing - Review & Editing.

Data availability

Data will be made available on request.

Declaration of competing interest

The authors declare that they have no known competing financial interests or personal relationships that could have appeared to influence the work reported in this paper.

Acknowledgements

This work was supported by the UK Research and Innovation Natural Environment Research Council as part of the NC-International programme [NE/X006247/1] delivering National Capability. We would like to acknowledge the creators of the Potential Natural Vegetation Map of East Africa; the creators and maintainers of the digital soil maps and covariate datasets held on the iSDAsoil webpage; Natural Earth for the Kenya shapefile (from the "1:10m Cultural Vectors" dataset); AfSIS for soil profile information, and the Food and Agriculture Organisation (FAO) for the soil type map, which were both used to generate the soil erodibility (RUSLE K-factor) map of Kenya. We would also like to thank the handling editor and anonymous reviewers for their feedback which have strengthened the quality of the manuscript.

Appendix A. Supplementary data

Supplementary data to this article can be found online at https://doi.org/10.1016/j.scitotenv.2023.161925.

References

Alewell, C., Borrelli, P., Meusburger, K., Panagos, P., 2019. Using the USLE: chances, challenges and limitations of soil erosion modelling. Int. Soil Water Conserv. Res. 7 (3), 203–225. https://doi.org/10.1016/j.iswcr.2019.05.004.

Alewell, C., Ringeval, B., Ballabio, C., Robinson, D.A., Panagos, P., Borrelli, P., 2020. Global phosphorus shortage will be aggravated by soil erosion. NatureCommunications 11 (1). https://doi.org/10.1038/s41467-020-18326-7.

Amundson, R., Berhe, A.A., Hopmans, J.W., Olson, C., Sztein, A.E., Sparks, D.L., 2015. Soil and human security in the 21st century. Science 348 (6235), 1261071. https://doi.org/10.1126/science.1261071.

Arnáez, J., Lana-Renault, N., Lasanta, T., Ruiz-Flaño, P., Castroviejo, J., 2015. Effects of farming terraces on hydrological and geomorphological processes. A review. Catena 128, 122–134. https://doi.org/10.1016/j.catena.2015.01.021.

Bagarello, V., Di Stefano, C., Ferro, V., Giordano, G., Iovino, M., Pampalone, V., 2012. Estimating the USLE soil erodibility factor in Sicily, South Italy. Appl. Eng. Agric. 28 (2), 199–206.

Bakker, M.M., Govers, G., Kosmas, C., Vanacker, V., Van Oost, K., Rounsevell, M., 2005. Soil erosion as a driver of land-use change. Agric. Ecosyst. Environ. 105 (3), 467–481. https://doi.org/10.1016/j.agee.2004.07.009.

Batista, P.V.G., Evans, D.L., Cândido, B.M., Fiener, P., 2022. Going down the rabbit hole: an exploration of the soil erosion feedback system. EGUsphere 1–32. https://doi.org/10.5194/egusphere-2022-181 preprint.

Batjes, N.H., 1996. Global assessment of land vulnerability to water erosion on a 1/2° by 1/2° grid. Land Degrad. Dev. 7 (4), 353–365. https://doi.org/10.1002/(SICI)1099-145X(199612)7:4<353::AID-LDR239>3.0.CO;2-N.

Benavidez, R., Jackson, B., Maxwell, D., Norton, K., 2018. A review of the revised universal soil loss equation RUSLE: with a view to increasing its global applicability and improving soil loss estimates. Hydrol. Earth Syst. Sci. 22 (11), 6059–6086.

Benkobi, L., Trlica, M.J., Smith, J.L., 1994. Evaluation of a refined surface cover subfactor for use in RUSLE. J. Range Manag. 47 (1), 74–78. https://doi.org/10.2307/4002845.

Borrelli, P., Robinson, D.A., Fleischer, L.R., Lugato, E., Ballabio, C., Alewell, C., Meusburger, K., Modugno, S., Schütt, B., Ferro, V., Bagarello, V., Van Oost, K., Montanarella, L., Panagos, P., 2017. An assessment of the global impact of 21st century land use change on soil erosion. NatureCommunications 8 (1). https://doi.org/10.1038/s41467-017-02142-7.

Borrelli, P., Robinson, D.A., Panagos, P., Lugato, E., Yang, J.E., Alewell, C., Wuepper, D., Montanarella, L., Ballabio, C., 2020. Land use and climate change impacts on global soil erosion by water (2015-2070). Proceedings of the National Academy of Sciences of the United States of America 117 (36), 21994–22001. https://doi.org/10.1073/pnas.2001403117.

David, W.P., 1988. Soil and water conservation planning: policy issues and recommendations. J.Philipp. Dev. 15 (1), 47–84.

Deng, C., Zhang, G., Liu, Y., Nie, X., Li, Z., Liu, J., Zhu, D., 2021. Advantages and disadvantages of terracing: a comprehensive review. Int. Soil Water Conserv. Res. 9 (3), 344–359. https://doi.org/10.1016/j.iswcr.2021.03.002.

Dietrich, W.E., Dunne, T., 1978. Sediment budget for a small catchment in mountainous terrain. Z. Geomorphol. 29, 191–206.

Estrada-Carmona, N., Harper, E.B., DeClerck, F., Fremier, A.K., 2017. Quantifying model uncertainty to improve watershed-level ecosystem service quantification: a global sensitivity analysis of the RUSLE. Int. J. Biodivers. Sci. Ecosyst. Serv. Manag. 13 (1), 40–50. https://doi.org/10.1080/21513732.2016.1237383.

Evans, D.L., Quinton, J.N., Davies, J.A.C., Zhao, J., Govers, G., 2020. Soil lifespans and how they can be extended by land use and management change. Environ. Res. Lett. 15 (9). https://doi.org/10.1088/1748-9326/aba2fd.

FAO, 1977. FAO/UNESCO Soil Map of the World. . https://www.fao.org/soils-portal/data-hub/soil-maps-and-databases/faounesco-soil-map-of-the-world/en/.

FAO, ITPS, 2015. Status of the World's Soil Resources (SWSR) - Main Report.

Feddema, J.J., Oleson, K.W., Bonan, G.B., Mearns, L.O., Buja, L.E., Meehl, G.A., Washington, W.M., 2005. Atmospheric science: the importance of land-cover change in simulating future climates. Science 310 (5754), 1674–1678. https://doi.org/10.1126/science.1118160.

Feeney, C.J., Chiverrell, R.C., Smith, H.G., Hooke, J.M., Cooper, J.R., 2020. Modelling the decadal dynamics of reach-scale river channel evolution and floodplain turnover in CAESAR-lisflood. Earth Surf. Process. Landf. 45 (5), 1273–1291. https://doi.org/10.1002/esp.4804.

Feeney, C.J., Cosby, B.J., Robinson, D.A., Thomas, A., Emmett, B.A., Henrys, P., 2022. Multiple soil map comparison highlights challenges for predicting topsoil organic carbon concentration at national scale. Sci. Rep. 12, 1379. https://doi.org/10.1038/s41598-022-05476-5.

Fenta, A.A., Tsunekawa, A., Haregeweyn, N., Poesen, J., Tsubo, M., Borrelli, P., Panagos, P., Vanmaercke, M., Broeckx, J., Yasuda, H., Kawai, T., Kurosaki, Y., 2020. Land susceptibility to water and wind erosion risks in the East Africa region. Sci. Total Environ. 703, 135016. https://doi.org/10.1016/j.scitotenv.2019.135016.

García-Ruiz, J.M., Beguería, S., Nadal-Romero, E., González-Hidalgo, J.C., Lana-Renault, N., Sanjuán, Y., 2015. A meta-analysis of soil erosion rates across the world. Geomorphology 239, 160–173. https://doi.org/10.1016/j.geomorph.2015.03.008.

Guya, F.J., 2019. Intrinsic and extrinsic sources of phosphorus loading into the Nyando River, Kenya. Lakes Reserv. Res. Manag. 24 (4), 362–371. https://doi.org/10.1111/lre.12289.

Hartemink, A.E., Veldkamp, T., Bai, Z., 2008. Land cover change and soil fertility decline in tropical regions. Turk. J. Agric. For. 32 (3), 195–213.

Hengl, T., Miller, M.A.E., Križan, J., Shepherd, K.D., Sila, A., Kilibarda, M., Antonijević, O., Glušica, L., Dobermann, A., Haefele, S.M., McGrath, S.P., Acquah, G.E., Collinson, J., Parente, L., Sheykhmousa, M., Saito, K., Johnson, J.M., Chamberlin, J., Silatsa, F.B.T., Crouch, J., 2021. African soil properties and nutrients mapped at 30 m spatial resolution using two-scale ensemble machine learning. Sci. Rep. 11 (1), 1–18. https://doi.org/10.1038/s41598-021-85639-y.

Humphrey, O.S., Osano, O., Aura, C.M., Marriott, A.L., Dowell, S.M., Blake, W.H., Watts, M.J., 2022. Evaluating spatio-temporal soil erosion dynamics in the Winam Gulf catchment, Kenya for enhanced decision making in the land-lake interface. Sci. Total Environ. 815, 151975. https://doi.org/10.1016/j.scitotenv.2021.151975.

iSDA, 2022. iSDAsoil. ISDA-Africa. https://www.isda-africa.com/isdasoil/.

Jena, P.R., De Groote, H., Nayak, B.P., Hittmeyer, A., 2021. Evolution of fertiliser use and its impact on maize productivity in Kenya: evidence from multiple surveys. Food Security 13 (1), 95–111. https://doi.org/10.1007/s12571-020-01105-z.

Jenny, H., 1941. Factors of Soil Formation: A System of Quantitative Pedology. Dover Publications.

Kagabo, D.M., Stroosnijder, L., Visser, S.M., Moore, D., 2013. Soil erosion, soil fertility and crop yield on slow-forming terraces in the highlands of Buberuka, Rwanda. Soil Tillage Res. 128, 23–29. https://doi.org/10.1016/j.still.2012.11.002.

Kassam, A.H., van Velthuizen, H.T., Mitchell, A.J.B., Fischer, G.W., Shah, M.M., 1991. Agro-Ecological land resources assessment for agricultural development planning: a case study of Kenya. Technical Annex 2: Soil Erosion and Productivity. https://www.fao.org/3/t0733e/T0733E00.htm.

Kinnell, P.I.A., 2005. Why the universal soil loss equation and the revised version of it do not predict event erosion well. Hydrol. Process. 19 (3), 851–854. https://doi.org/10.1002/hyp.5816.

Labrière, N., Locatelli, B., Laumonier, Y., Freycon, V., Bernoux, M., 2015. Soil erosion in the humid tropics: a systematic quantitative review. Agric. Ecosyst. Environ. 203, 127–139. https://doi.org/10.1016/j.agee.2015.01.027.

Lal, R., 2003. Soil erosion and the global carbon budget. Environ. Int. 29 (4), 437–450. https://doi.org/10.1016/S0160-4120(02)00192-7.

Liniger, H.P., 1992. Water and soil conservation in the semi-arid highlands northwest of Mount Kenya. In: Hurni, H., Tato, K. (Eds.), Erosion, Conservation and Small Scale Farming. Geographica Bernesia, pp. 483–504.

Lugato, E., Smith, P., Borrelli, P., Panagos, P., Ballabio, C., Orgiazzi, A., Fernandez-Ugalde, O., Montanarella, L., Jones, A., 2018. Soil erosion is unlikely to drive a future carbon sink in Europe. ScienceAdvances 4 (11), eaau3523. https://doi.org/10.1126/sciadv.aau3523.

May, L., Dobel, A.J., Ongore, C., 2022. Controlling water hyacinth (Eichhornia crassipes (Mart.) Solms): a proposed framework for preventative management. Inland Waters 12 (1), 163–172. https://doi.org/10.1080/20442041.2021.1965444.

Maynard, J.J., Yeboah, E., Owusu, S., Buenemann, M., Neff, J.C., Herrick, J.E., 2022. Accuracy of regional-to-global soil maps for on-farm decision making: are soil maps "good enough"? EGUsphere 1–35. https://doi.org/10.5194/egusphere-2022-246 preprint.

McCool, D.K., Renard, K.G., 1990. Water erosion and water quality. Advances in Soil Science. Springer, pp. 175–185.

MEA, 2005. Ecosystems and Human Well-being: Synthesis.

Meadows, T., 2014. Forecasting Long-term Sediment Yield From the Upper North Fork Toutle River, Mount St Helens, USA. University of Nottingham. http://eprints.nottingham.ac.uk/27800/.

Montanarella, L., Pennock, D.J., McKenzie, N., Badraoui, M., Chude, V., Baptista, I., Mamo, T., Yemefack, M., Aulakh, M.S., Yagi, K., Hong, S.Y., Vijarnsorn, P., Zhang, G.L., Arrouays, D., Black, H., Krasilnikov, P., Sobocká, J., Alegre, J., Henriquez, C.R., Vargas, R., 2016. World's soils are under threat. Soil 2 (1), 79–82. https://doi.org/10.5194/soil-2-79-2016.

Montgomery, D.R., 2007. Soil erosion and agricultural sustainability. Proceedings of the National Academy of Sciences of the United States of America 104 (33), 13268–13272. https://doi.org/10.1073/pnas.0611508104.

Mosier, S., Córdova, S.C., Robertson, G.P., 2021. Restoring soil fertility on degraded lands to meet food, fuel, and climate security needs via perennialization. Front. Sustain. Food Syst. 5, 706142. https://doi.org/10.3389/fsufs.2021.706142.

Mulinge, W., Gicheru, P., Murithi, F., Maingi, P., Kihiu, E., Kirui, O.K., Mirzabaev, A., 2016. Economics of land degradation and improvement in Kenya. In: Nkonya, E., Mirzabaev, A., von Braun, J. (Eds.), Economics of Land Degradation and Improvement - A Global Assessment for Sustainable Development. Springer, pp. 471–498.

Muriuki, J.P., Macharia, P.N., 2011. Inventory and analysis of existing soil and water conservation practices in inventory and analysis of existing soil and water conservation practices in the Upper Tana, Kenya. Green Water Credits Report, p. 12.

Earth, Natural, 2022. 1:10m cultural vectors: admin 0 - countries. https://www.naturalearthdata.com/downloads/10m-cultural-vectors/.

Nyawacha, S.O., Meta, V., Osio, A., 2021. Spatial temporal mapping of spread of water hyacinth in winum gulf, Lake Victoria. Int. Arch. Photogramm. Remote Sens. Spat. Inf. Sci. - ISPRS Arch. 43, 341–346. https://doi.org/10.5194/isprs-archives-XLIII-B3-2021-341-2021 B3–2021.

Oreskes, N., 1998. Evaluation (not validation) of quantitative models. Environ. Health Perspect. 106 (Suppl. 6), 1453–1460. https://doi.org/10.1289/ehp.98106s61453.

Oreskes, N., Shrader-Frechette, K., Belitz, K., 1994. Verification, validation, and confirmation of numerical models in the earth sciences. Science 263 (5147), 641–646. https://doi.org/10.1126/science.263.5147.641.

Panagos, P., Borrelli, P., Poesen, J., Ballabio, C., Lugato, E., Meusburger, K., Montanarella, L., Alewell, C., 2015. The new assessment of soil loss by water erosion in Europe. Environ. Sci. Policy 54, 438–447. https://doi.org/10.1016/j.envsci.2015.08.012.

Pasculli, A., Audisio, C., 2015. Cellular automata modelling of fluvial evolution: real and parametric numerical results comparison along river pellice (NW Italy). Environ. Model. Assess. 20 (5), 425–441. https://doi.org/10.1007/s10666-015-9444-8.

Pimentel, D., Burgess, M., 2013. Soil erosion threatens food production. Agriculture (Switzerland) 3 (3), 443–463. https://doi.org/10.3390/agriculture3030443.

Power, J.F., Sandoval, F.M., Ries, R.E., Merrill, S.D., 1981. Effects of topsoil and subsoil thickness on soil water content and crop production on a disturbed soil. Soil Sci. Soc. Am. J. 45 (1), 124–129. https://doi.org/10.2136/sssaj1981.03615995004500010027x.

Prăvălie, R., 2021. Exploring the multiple land degradation pathways across the planet. Earth Sci. Rev. 220 (May). https://doi.org/10.1016/j.earscirev.2021.103689.

Quinton, J.N., Govers, G., Van Oost, K., Bardgett, R.D., 2010. The impact of agricultural soil erosion on biogeochemical cycling. Nat. Geosci. 3 (5), 311–314. https://doi.org/10.1038/ngeo838.

Renard, K.G., Foster, G.R., Weesies, G.A., McCool, D.K., Yoder, D.C., 1997. Predicting soil erosion by water: a guide to conservation planning with the revised universal soil loss equation (RUSLE). Agriculture Handbook 703, 404.

Rickson, R.J., 2014. Can control of soil erosion mitigate water pollution by sediments? Sci. Total Environ. 468–469, 1187–1197. https://doi.org/10.1016/j.scitotenv.2013.05.057.

Rutebuka, J., Munyeshuli Uwimanzi, A., Nkundwakazi, O., Mbarushimana Kagabo, D., Mbonigaba, J.J.M., Vermeir, P., Verdoodt, A., 2021. Effectiveness of terracing techniques for controlling soil erosion by water in Rwanda. J. Environ. Manag. 277, 111369. https://doi.org/10.1016/j.jenvman.2020.111369.

Sanderman, J., Berhe, A.A., 2017. Biogeochemistry: the soil carbon erosion paradox. Nat. Clim. Chang. 7 (5), 317–319. https://doi.org/10.1038/nclimate3281.

Smaling, E.M.A., Nandwa, S.M., Janssen, B.H., 2015. Soil fertility in Africa is at stake. Replenishing Soil Fertility in Africa. 51, pp. 47–61. https://doi.org/10.2136/sssaspecpub51.c2.

Strauss, P., Swoboda, D., Blum, W.E.H., 2003. How effective is mulching and minimum tillage to control runoff and soil loss?—a literature review. Proceedings of the Conference on 25 Years of Assessment of Erosion, pp. 545–550.

Taye, G., Poesen, J., Vanmaercke, M., Van Wesemael, B., Martens, L., Teka, D., Nyssen, J., Deckers, J., Vanacker, V., Haregeweyn, N., Hallet, V., 2015. Evolution of the effectiveness of stone bunds and trenches in reducing runoff and soil loss in the semi-arid Ethiopian highlands. Z. Geomorphol. 59 (4), 477–493. https://doi.org/10.1127/zfg/2015/0166.

Taye, G., Vanmaercke, M., Poesen, J., Van Wesemael, B., Tesfaye, S., Teka, D., Nyssen, J., Deckers, J., Hare., 2017. Determining RUSLE P- and C-factors for stone bunds and trenches in rangeland and cropland. Land Degrad. Dev. 29 (3), 812–824. https://doi.org/10.1002/ldr.2814.

van Breugel, P., Kindt, R., Lilleso, J.B.P., Bingham, M., Demissew, S., Dudley, C., Friis, I., Gachathi, F., Kalema, J., Mbago, F., Moshi, H.N., Mulumba, J., Namaganda, M., Ndangalasi, H.J., Ruffo, C.K., Vedaste, M., Jamnadass, R., Graudal, L., 2015. Potential Natural Vegetation Map of Eastern Africa (Burundi, Ethiopia, Kenya, Malawi, Rwanda, Tanzania, Uganda and Zambia) (2.0). Forest and Landscape (Denmark) and World Agroforestry Centre (ICRAF).

Van Oost, K., Quine, T.A., Govers, G., De Gryze, S., Six, J., Harden, J.W., Ritchie, J.C., McCarty, G.W., Heckrath, G., Kosmas, C., Giraldez, J.V., Marques Da Silva, J.R., Merckx, R., 2007. The impact of agricultural soil erosion on the global carbon cycle. Science 318 (5850), 626–629. https://doi.org/10.1126/science.1145724.

Watene, G., Yu, L., Nie, Y., Zhang, Z., Hategekimana, Y., Mutua, F., Ongoma, V., Ayugi, B., 2021. Spatial-temporal variability of future rainfall erosivity and its impact on soil loss risk in Kenya. Appl. Sci. 11 (21), 9903. https://doi.org/10.3390/app11219903.

Wischmeier, W.H., Smith, D.D., 1978. Predicting rainfall erosion losses: a guide to conservation planning. Agriculture Handbook. 537, p. 69.

Wuepper, D., Borrelli, P., Panagos, P., Lauber, T., Crowther, T., Thomas, A., Robinson, D.A., 2021. A 'debt' based approach to land degradation as an indicator of global change. Glob. Chang. Biol. 27 (21), 5407–5410. https://doi.org/10.1111/gcb.15830.

Zhao, W., Hua, T., Meadows, M.E., Pereira, P., 2021. Degradation debts accounting: a holistic approach towards land degradation neutrality. Glob. Chang. Biol. 27 (21), 5411–5413. https://doi.org/10.1111/gcb.15855.